

Graphene waveguide-integrated thermal infrared emitter

Nour Negm^{1,2}, Sarah Zayouna³, Shayan Parhizkar^{1,2}, Pen-Sheng Lin⁴, Po-Han Huang⁴, Stephan Suckow¹, Stephan Schröder³, Eleonora De Luca³, Flavia Ottonello Briano³, Arne Quellmalz⁴, Frank Niklaus⁴, Kristin B. Gylfason⁴, Max C. Lemme^{1,2}

¹AMO GmbH, Advanced Microelectronic Center Aachen, Otto-Blumenthal-Str. 25, Aachen, 52074, Germany

²Chair of Electronic Devices, RWTH Aachen University, Otto-Blumenthal-Str. 25, Aachen, 52074, Germany

³Senseair AB, Stationsgatan 12, Delsbo, 824 08, Sweden

⁴KTH Royal Institute of Technology, Stockholm, 100 44, Sweden

Email: suckow@amo.de, max.lemme@rwth.aachen.de / Phone: (+49) 241 8867 201

Introduction: Low-cost and easily integrable mid-infrared (MIR) sources are highly desired for photonic integrated circuits. Thermal incandescent MIR sources are widely used. They work by Joule heating, i.e. an electrical current through the emitter causes thermal emission according to Planck's law. Their simple design with only two contact pads makes them integrable with typical optoelectronic components in high-volume production flows. Graphene's emissivity is comparable to common metallic emitters. In contrast to the latter, graphene is transparent at MIR wavelengths, which enables placing large area graphene emitters in the evanescent field of integrated waveguides [1-2]. This enhances emission by near-field coupling directly into the waveguide mode, avoiding the mode-mismatch to free space. Here, we present the first experimental demonstration of a graphene emitter placed directly on a photonic waveguide, hence emitting directly into the waveguide mode.

Fabrication and Characterization: 50 nm high and 3 μm wide rib-waveguides were dry-etched into SOI substrates with 3 μm buried oxide and 220 nm top silicon. 40 nm palladium (Pd) contacts were evaporated and patterned by lift-off. Monolayer Graphene was wet-transferred on top of the contacts and waveguide, and patterned with oxygen plasma. 40 nm of aluminum oxide (Al_2O_3) were atomic layer deposited to encapsulate the graphene and then removed elsewhere wet-chemically. A schematic top view, cross section and SEM image of an emitter are shown in Fig. 1. An infrared camera with a wavelength range from 3 to 5 μm was positioned above the chip to detect the light at the emitter and the grating couplers (GCs), which were optimized for $\lambda = 4.2 \mu\text{m}$ (Fig. 2). The graphene was contacted via the metal pads with a source measure unit (SMU), which acted as a DC current source and voltage meter simultaneously. The samples were measured under ambient conditions with 10% to 20% humidity at 22°C.

Results: A DC current density of 0.45 mA/ μm was forced through a graphene emitter. This leads to high emission intensities at the emitter, the GC and the probe tips, the latter due to reflections (Fig. 3). The emission at the output GC of the waveguide clearly demonstrates the functionality of our concept. The emission intensity at the source is higher than at the output, because the light observed at the GC is subject to propagation losses and GC coupling losses. These were estimated to be -1 and -15 dB, respectively, based on cutback measurements (Fig. 4). The emission of and the voltage drop along an emitter operated at 0.2 mA/ μm DC were measured over time. After settling for ~ 16 mins, the temperature and voltage drop remained stable until the graphene emitter broke after ~ 54 min (Fig. 5). This limited DC stability requires further experiments, including AC measurements. During the settling time (6 to 16 min of operation) the voltage drop (= emitter resistance) increased. We attribute this to current-induced damage to parts of the graphene sheet or the graphene-metal contacts, which reduces the effective device width and increases the current density and thus the heating power (here: from 60 mW to 80 mW). Higher currents lead to devices breaking faster, with thermal runaway occurring between 250 mW and 350 mW before final breakdown (Fig. 6a). Two common breakdown points have been identified (inset of Fig. 5): the contact edge and the edge of the rib waveguide. The former is caused by the contact resistance. The latter may be caused by tension in the graphene suspended over the 50 nm step, or by hot spots in the suspended areas receiving less cooling by the substrate. The emitters may be functional up to 200 mW (Fig. 6a), where they reach a simulated temperature of 1400 K (Fig. 6b), which is close to the melting points of the materials used in these devices. Tab. 1 compares the performance of our emitters with current state of the art using conventional materials. They reach comparable temperatures, which is the most important parameter for thermal emitters, as their emitted power scales with the 4th power of temperature (T^4).

Conclusions: We successfully integrated graphene emitters into photonic waveguides. Their performance is on par with metallic thermal emitters, but graphene allows more efficient nearfield coupling at comparable temperatures.

Acknowledgements: This work has received funding from the European Union's Horizon 2020 research and innovation programme under grant agreements No 825272 (ULISSES) and No 101017186 (AEOLUS).

[1] Lawton *et al.*, *AIP Adv.*, vol. 4, p. 087139, (2014). [2] Schall *et al.*, *Opt. Express*, vol. 24, p. 7871, (2016).

[3] Luo *et al.*, *ACS Photonics*, vol. 6, p. 2117, (2019). [4] Miyoshi *et al.*, *Nat. Commun.*, vol. 9, p. 1279, (2018).

[5] Pyatkov *et al.*, *Beilstein J. Nanotech.*, vol. 8, p. 38, (2017). [6] Schröder *et al.*, *Microsys. Nanoeng.*, vol. 7, p. 87, (2021).

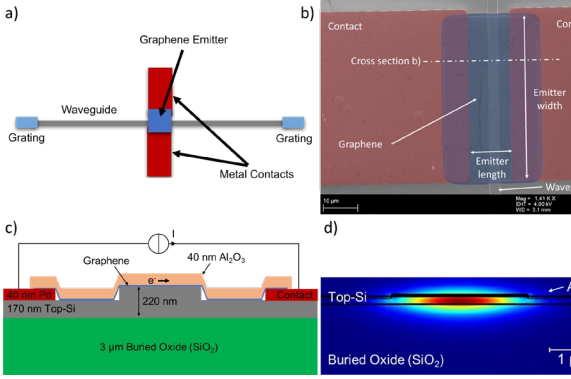


Fig. 1 Waveguide-integrated graphene-based thermal emitter a) Top view, and b) false-colored SEM image, before encapsulation. c) Cross section of the emitter after encapsulation. d) Electric field profile of the fundamental TE mode of the waveguide, calculated at $\lambda = 4.2 \mu\text{m}$ using Ansys Lumerical.

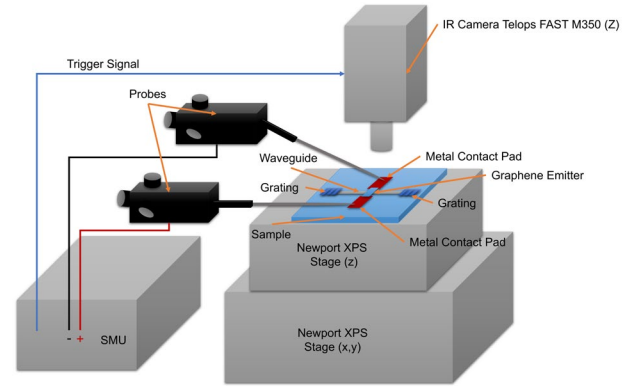


Fig. 2 Schematic of the MIR measurement setup, showing the components and connections to the integrated thermal emitter on the sample. In Fig. 3 the camera focusses on the emitter and one of the output grating couplers.

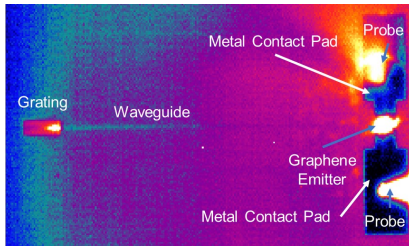


Fig. 3 MIR camera image of a thermal emitter heated by 185 mW, waveguide and grating coupler. The distance between grating coupler and emitter is 725 μm .

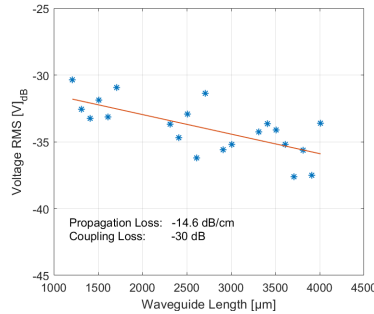


Fig. 4 Cutback plot of loss in dB versus length of different waveguides to determine the propagation (slope) and coupling losses (y-intercept) at $\lambda = 4.2 \mu\text{m}$.

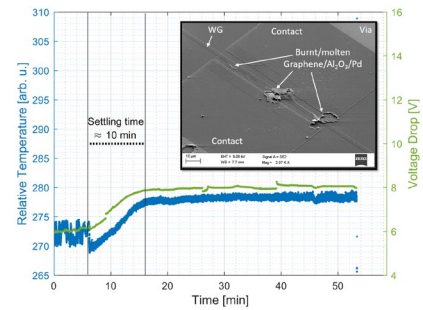


Fig. 5 Relative temperature, i.e. emission in arb. u., and voltage drop of an emitter driven with 0.2 mA/ μm , versus time. Inset: SEM image showing the device after breakdown.

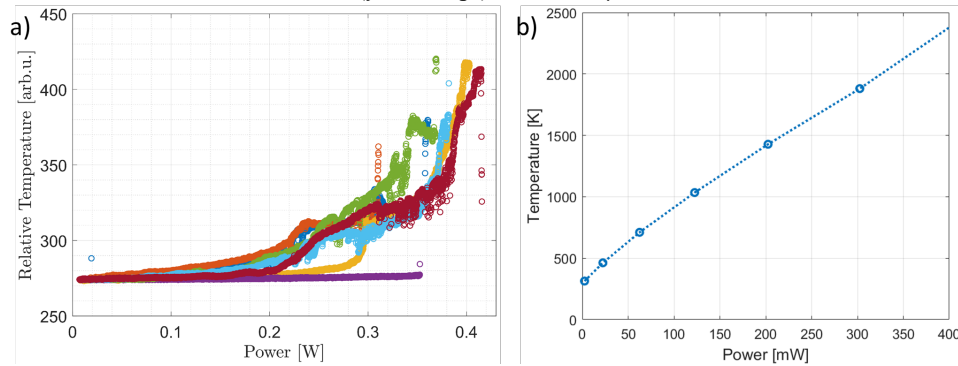


Fig. 6 a) Relative temperature, i.e. emission in arbitrary units, of several nominally identical emitters, versus input power. b) COMSOL simulation of graphene temperature versus input power.

Ref.	Material	Coupled to	Current	Voltage	Power Consumption	Emitting Area	Temperature	Speed	Lifetime
Here	Graphene monolayer	Waveguide	0.2 – 0.45 mA/ μm		60 – 200 mW	50 x 10 μm^2	700 – 1400 K*		54 min
[3]	Graphene	Free space	1x10 ⁸ A/cm ²		80 kW/cm ²		1600 K		
[4]	Graphene multilayer	Free space		8 V			750 K*	10 GHz (100 ns response time)	> 1000 h
[5]	CNT (3 – 100 μm^{-1})	Waveguide		1.5 – 10 V _{DC} & additional 2 – 3.3 V _{ripple}			1000 – 1500 K*	100 kHz – 2 GHz (decay time < 80 ps)	
[6]	Kanthal (FeCrAl)	Free space	150 – 200 mA	6.5 V	0.8 – 1 W	1 x 1 mm ²	700 – 1200 K	5 Hz	

Tab. 1 Comparison of the present work with the state of the art. Simulated values are marked by *.